P1.17 QUANTITATIVE PRECIPITATION FORECASTING OF WINTERTIME STORMS IN THE SIERRA NEVADA: SENSITIVITY TO THE MICROPHYSICAL PARAMETERIZATION

Ramesh K. Vellore, Vanda Grubišić*, and Arlen W. Huggins
Desert Research Institute, Reno, Nevada

1. INTRODUCTION

Precipitation is a highly variable meteorological quantity, which is the end product of complex chain of nonlinear physical processes occurring in the atmosphere over a variety of space and time scales. The spatial and temporal distribution of precipitation has significant socio-economic impact, namely in agriculture, water resources management, transportation, hydroelectric power production, and in various day-to-day activities of general population. The availability of high-skill short-term quantitative precipitation forecasts from regional numerical models could facilitate adjustment of activities to minimize losses and maximize gains. Quantitative precipitation forecasting (QPF) represents one of the most important, and most difficult areas in numerical weather forecasting. The QPF skill of operational forecasting models has been traditionally low, and the improvements in QPF have been slow compared to other forecasted variables. The combination of low forecasting skill and high socio-economic impact has led the scientific community of the U.S. Weather Research Program (USWRP) to consider the improvements in QPF as the problem of the highest priority (Fristch et al. 1998).

In spite of sophisticated high-resolution regional mesoscale models and advanced computing power, achieving accurate short-term precipitation forecasting has been a challenging task. In QPF, there are various sources of error including the representation of local properties such as orography and landuse, physical processes within clouds, model initialization errors of various fields, particularly water substance quantities, and the spatial resolution (Montani et al. 1999; Bruintjes et al. 1994; Gaudet and Cotton 1998). The representation of cloud microphysical processes can have a profound influence on the amount, spatial distribution and occurrence of precipiation, especially for orographic precipitation events in complex mountaineous terrain (Schultz et al. 2002).

Major mountain ranges in the western U.S. such as the Sierra Nevada and Washington Cascades receive large amounts of precipitation from the frequent passage of storms from the Pacific Ocean during winter months. The climatology of winter storms in the Sierra Nevada shows that heavy precipitation events contribute a large fraction of total winter precipitation (Cayan and Riddle 1993). Sierra Nevada, the north-northwest to south-southeast oriented mountain range with an approximate length of 600 km and a half width of 100 km, lies nearly perpendicular to the path of Pacific storms. This mountain range is an ideal environment suited for studies of orographic precipitation processes due to its gentle (2%) upwind slope and the absence of larger mountains upstream (aside from ∼300 m high Coastal Range). The quasi-two dimensional mountain range slopes up uniformly from the Central Valley of California (at 0.1 km ASL) to approximately 2.2 km ASL over a horizontal distance of 100 km. There is a very small number of high passes that interrupt the compact ridgeline but a fairly large number of deep river valleys on the western slope oriented perpendicular to the mountain range (Fig 1). The heavy precipitation on the western slopes of the Sierra Nevada is caused mainly by orographic lifting of the oceanic inflow of air at the upstream slopes of the mountain range. The precipitation distribution varies significantly in the west-east direction with a typical maximum precipitation 10–20 km upstream of the crest, accompanied by a strong shadowing effect on the lee side (Rauber 1992).

Recent modeling studies have suggested that precipitation structures are better resolved at higher spatial resolutions in mesoscale models. The noted discrepancies between the observed and model-predicted precipitation point to an over-prediction of precipitation on the windward slopes and under-estimation on the lee slopes

* *Corresponding author's address:* Dr. Vanda Grubišić, Desert Research Institute, Division of Atmospheric Sciences, 2215 Raggio Pkwy, Reno, NV 89512–1095; e-mail: grubisic@dri.edu

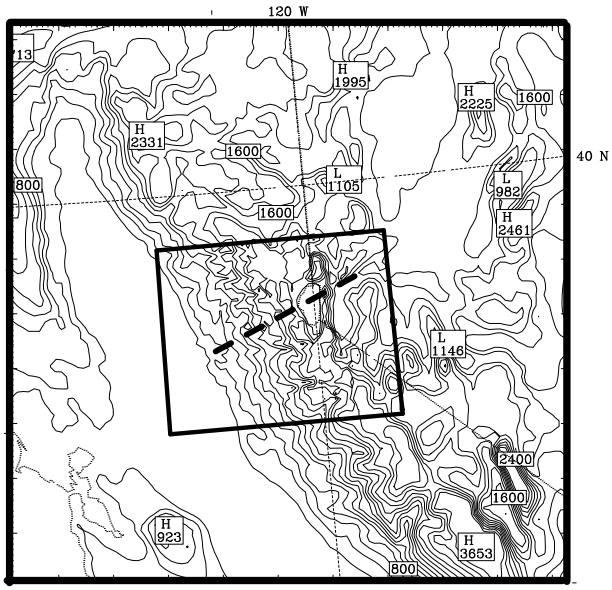

Figure 1: The representation of orography within one of the nested domains of the MM5 simulations with horizontal resolution of 4.5 km. The inset rectangular marks the boundary of the innermost domain with horizontal resolution of 1.5 km. Terrain contours are shown at 200 m interval. A dashed line crossing the Sierra Nevada marks the location of the vertical cross section shown in Figs. 3 and **??**.

(Colle and Mass 2000). Therefore, the increased resolution alone appears insufficient to address the challenges of improving QPF. Recent QPF studies have also emphasized the need for better understanding and representation of microphysical processes in regional mesoscale models in complex terrain (Schultz et al. 2002; Colle et al. 2002). In this paper, we report on a detailed investigation of the QPF skill of a mesoscale model for winter storms in the Sierra Nevada, and its dependence on the choice of the microphysical scheme. The goal of this study is to diagnose what parts of the existing microphysical schemes require most improvement.

2. NUMERICAL MODEL

The numerical model chosen for this study is NCAR/Penn State MM5, a nonhydrostatic model with a multiple nesting capability and a full suite of physical parameterizations (Grell et al. 1994). High resolution numerical simulations were carried out by employing two-way interactive nesting on stationary triple nested domains in which horizontal grid increments are 13.5, 4.5, and 1.5 km. In the outer domain, the horizontal grid increment is 40.5 km. Thirty one unequally spaced atmospheric layers are chosen between the surface and 100 hPa, with 5 layers within the lowest 1 km of the domain. The model topography and landuse data in the two innermost domains were obtained by interpolating the 30-sec (0.9 km) U.S. Geological Survey data sets to the model grid resolution. At the horizontal resolution of 4.5-km and 1.5-km, major features of local orography are well resolved. Initial model atmospheric conditions were obtained by interpolating the NCAR/NCEP global reanalyses (2.5° lat ×2.5° long resolution) to the model grids. The reanalysis fields were combined with available surface and upper-air observations, and were also used to update the lateral boundary conditions every 6 hours during the model prognosis.

The model simulations were initialized 12 hours ahead of the period of interest, and carried out on all domains simultaneously. As the focus of this study is the sensitivity of wintertime precipitation forecasts on the choice of the microphysical parameterization, several schemes available in MM5 were used. The experiments were varied only in the the choice of the microphysical parameterization. The selected choices in this study are : (1) Dudhia's ice scheme (DUDH; Dudhia 1989), a simple ice-scheme modification of the Hsie et al. (1984) warm-rain scheme, which allows no supercooled water below 0°C and assumes that melting of ice occurs immediately above 0°C, (2) Reisner's mixed-phase scheme (REIS; Reisner et al. 1998), which permits existence of supercooled water below 0°C, and in which melting of ice does not occur immediately above 0°C, (3) Goddard's mixed-phase scheme (GSFC; Tao and Simpson 1993), which predicts liquid phase categories such as cloud water and rain using Kessler type parameterization (Kessler 1969), and ice phase categories such as cloud ice, snow and hail/graupel following the bulk parameterization of Lin et al. (1983), and (4) Schultz's mixed-phase scheme (SCHUL; Schultz 1995), which predicts the ice or water substance in a certain production sequence.

3. VERIFICATION DATA SET AND METHODS

The observational dataset used for model verification consists of a selected number of high-impact precipitation events from the 1980's, documented during the Sierra Co-operative Pilot Project (SCPP). This field project, administered by the U.S. Bureau of Reclamation, was designed to document physical processes associated with orographic winter

Start Date–Time (UTC)	End Date–Time (UTC)	Maximum Precipitation (inches/day)
820113–1300	820216–2000	3.96
821217–0500	821218–0100	3.08
830330–2200	830331–1600	2.61
860212–0400	860213–1500	3.41
860214–0000	860222–0000	4.08
870103–1100	870104–0500	4.07

Table 1: SCPP storms selected for QPF validation. The precipitation maximum in the third column reflects the storm maximum precipitation recorded at Sheridan, California (38.875° N, 121.375° W, 60 m ASL) divided by the storm length (in days).

storms, with the goal of verifying the weather modification technology employed in the central Sierra Nevada (Reynolds and Dennis 1986). During SCPP, precipitation measurements were obtained at 15-min intervals at a number of stations, the majority of which lie on the windward slopes. We have used the SCPP data to verify model forecasts for storms periods listed in Table 1. In order to generate a denser observational grid for determining the statistical skill scores of precipitation forecasts in our study, the SCPP precipitation data was supplemented with additional data from the archives of the Western Regional Climate Center (WRCC) at the Desert Research Institute (DRI). Figure 2 shows the observational data points used in verification.

For verification, the model-predicted precipitation amounts within the two innermost model domains obtained for the four selected microphysical schemes were compared with available observations. To obtain the model-predicted and measured data at the same spatial locations, the MM5 precipitation forecasts were interpolated from the regular model grid to the precipitation gauge locations using Cressman (1959) method. The statistical analysis employed in the verification is based on a contingency table (Table 2), in which individual elements represent a number of events (or stations) for which forecasted and measured precipitation amounts were found to fall within certain threshold classes for a given 24-h forecast period. The threshold precipitation classes are 0.01–0.5 in, 0.5–1.5 in, and 1.5–2.5 in for light, moderate, and heavy precipitation, respectively, which were determined based on the frequency distribution of observations and model forecasts in each precipitation class. Two main statistical scores that were calculated from the contingency table and are discussed here are bias (BIAS) and Heidke skill score (HSS). The scores were calculated for the entire set of observational data points contained within a circle 120 km in radius centered on the Sierra crest as well as separately for the upwind and lee-side locations contained within circular regions 50 km in radius placed on each side of the Sierra crestline (Fig 2).

	Observed (**Yes**)	Observed (**No**)
Forecast (**Yes**)	Hits (A)	False Alarm (B)
Forecast (**No**)	Misses (C)	Correct Negatives (D)

Table 2: Contingency Table

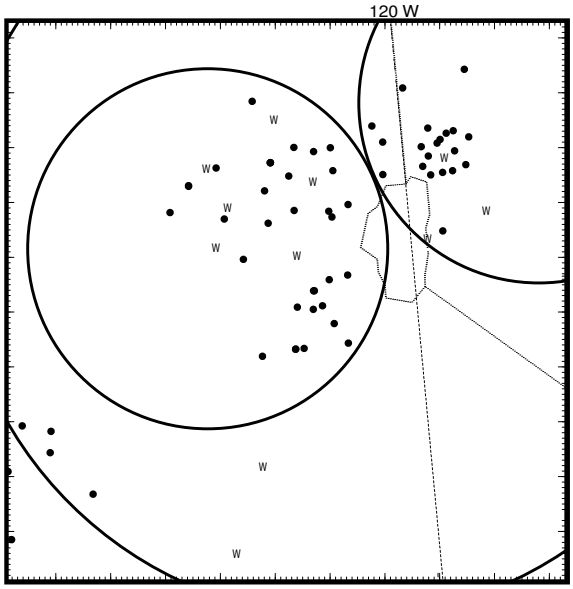

Figure 2: The innermost MM5 domain with verification data points for 12–13 February 1986 storm. The verification points include the SCPP gauge locations (solid circles) as well as additional stations from the WRCC archives (labeled as W). One large circle of 120 km radius and two smaller ones of 50 km radius on the windward and lee sides mark the domains of model verification.

The definition of bias is

$$BIAS \equiv \frac{F}{O} = \frac{A+B}{A+C}$$

where $N = A + B + C + D$ is the total number of observations, $F = A + B$ is the number of points

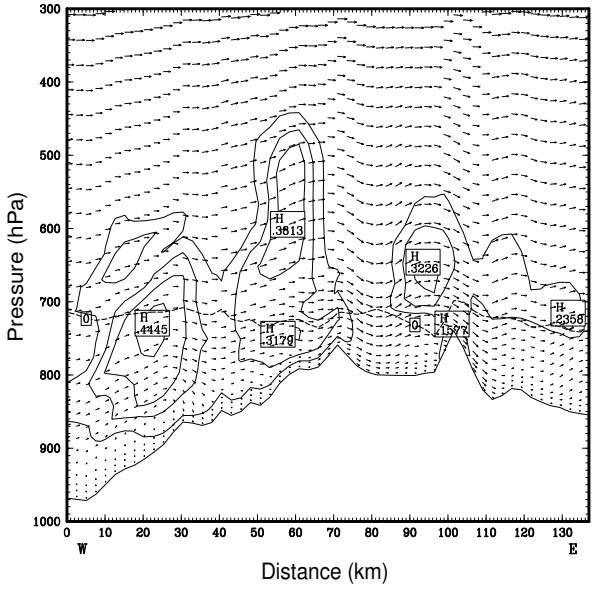

Figure 3: Winds (maximum vector length 40 ms^{-1}) and cloud water mixing ratio (contour interval 0.1 g kg^{-1}) in the 140 km long east-west vertical cross-section (cf. Fig. 1) from REIS simulation for 13 February 1986 at 00 UTC. Dashed thick line indicates the altitude of the freezing level.

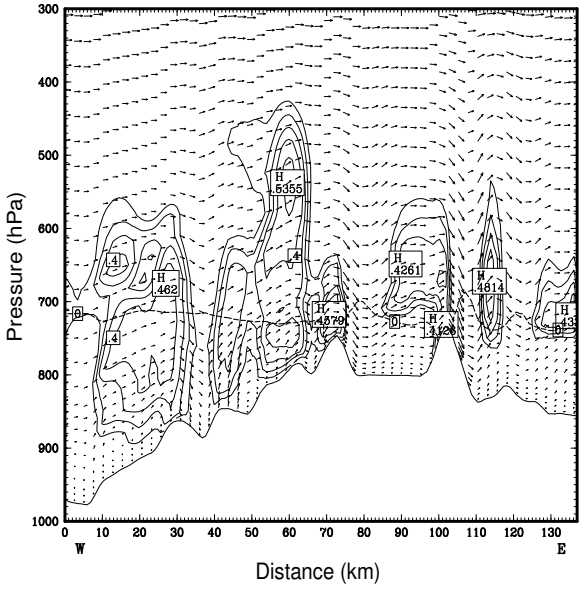

Figure 4: As in Fig. 3, but for the 1.5-km domain. Maximum vector length is 50 ms^{-1}.

in which the forecasted precipitation amount is in a given precipitation class, and $O = A + C$ is the number of points in which the observed precipitation falls within a given class. BIAS indicates how well the model predicts the frequency of occurrence of a given precipitation class. As a perfect forecasting system produces only A and D, the perfect score for BIAS is equal to unity. BIAS score of less than 1 indicates that the event was predicted fewer times than it was observed (under-prediction) and vice versa. Another commonly used simple verification index of categorical forecasts is threat score (TS), which is equal to the number of hits divided by the total number of occurrences in which the event was forecasted and/or observed ($TS = A/(A+B+C)$). TS is quite sensitive to the number of hits, and is not affected by correct negatives. As it has been shown that the omission of correct negatives produces biased scores in rare-event situations such as heavy precipitation (Marzban et al. 1998), instead of TS we use HSS, which measures the skill of forecast in predicting the correct precipitation class relative to a particular standard such as the forecast based upon random chance. HSS follows the form of a generic skill score based on the hit rate ($= (A+D)/N$), as the basic accuracy measure (Wilks 1995). HSS is defined as

$$HSS \equiv \frac{2(AD - BC)}{(A+C)(C+D) + (A+B)(B+D)} .$$

Perfect forecasts receive the scores of unity, forecasts equivalent to the reference forecast obtain the zero score, and forecasts worse than the reference forecast are assigned negative scores.

4. RESULTS

In the following, we limit our discussions to a subset of four winter storms from Table 1. The selected storms are 17–18 December 1982, 30–31 March 1983, 12–13 February 1986, and 3–4 January 1987. The common feature of these four storms is that they were embedded in a relatively strong southwesterly airflow coming from the Pacific (Rauber, 1992; Hemmer et al. 1987). Among these, 12–13 February 1986 storm was the strongest with continuous precipitation in the verification area during the entire period.

At the horizontal resolution of 4.5 and 1.5 km, the cloud dynamics is well resolved and the precipitation is primarily produced by microphysical schemes. The potential for enhanced orographic precipitation in winter storms is usually associated

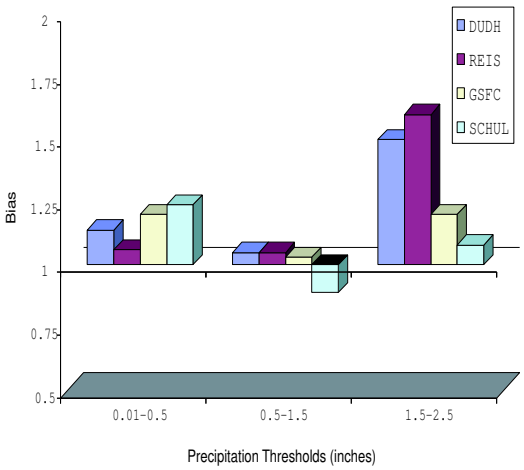

Figure 5: Bias scores for the defined precipitation classes (in) for different microphysical schemes for the 4.5-km model domain.

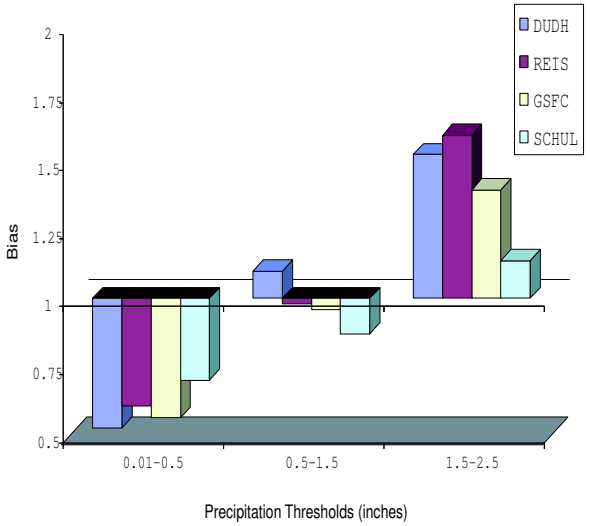

Figure 6: As in Fig. 5 but for the 1.5-km domain.

with a large cloud water content. As an illustration of the model predictions, in Figs. 3 and 4 we show the forecasted cloud water mixing ratio using REIS scheme for 12–13 February 1986 storm in the two innermost model domains along a vertical cross-section passing over the Sierra Nevada (cf. Fig. 1). It is apparent that large amount of cloud water, which gets converted to precipitation by various microphysical processes, is predicted on the windward slopes. This amount is larger at the higher resolution, particularly around well-resolved model terrain peaks.

In the computation of the QPF skill scores, the 24-h precipitation accumulations from these four storms were grouped together as a number of observations in each precipitation class was fairly small for individual storms. The same subset of observations in the two innermost domains was used for all four storms. The percentage of observations in the moderate precipitation class for these storms is considerably larger than in the other classes on both the upwind and lee sides. The scores were calculated for the entire set of observational data points as well as separately for the upwind and lee side.

In considering both the upwind and downwind sides together, the model displays the highest skill in forecasting the moderate amounts of precipitation regardless of the choice of the microphysical scheme. This conclusion is based not just on the BIAS and HSS scores shown in Figs. 5–8 but on a number of other scores such as TS, threshold root-mean-square errors and threshold bias. Comparing the statistical scores for the two innermost model domains, it is apparent that increasing the horizontal resolution does not automatically lead to the improvement in the skill scores. The increase in the horizontal resolution affects most significantly the light precipitation class, leading to a reduction in BIAS from 1.2 to 0.6 (average for all schemes), hit rate and reference forecast, thereby increasing HSS. This reduction in BIAS stems primarily from the lee side where the frequency of precipitation forecast is much smaller than observed in this class.

Looking at the windward and lee sides separately, we find a tremendous difference between the 24-h area-averaged precipitation amounts, both the model-predicted and observed (not shown here). Irrespective of the choice of the microphysical scheme, the model-predicted 24-h total precipitation is larger than observed on both sides. On the windward side, the model predicted amount is nearly 2.5 times the observed, compared to close to 1.3 times on the lee side. This over-prediction results primarily from the over-prediction in the heavy precipitation class, which is true on both sides of the range irrespective of the choice of the microphysical scheme. For the light and moderate precipitation classes, the model shows a better QPF skill on the windward side compared to the lee side. We find a good agreement between the predicted and observed frequency of precipitation in the light and moderate precipitation classes resulting in good BIAS (0.9–1) and HSS (positive) scores on the windward side. On the lee side, the model displays a much worse QPF skill in these categories. For all schemes except REIS, HSS scores are negative for both of these

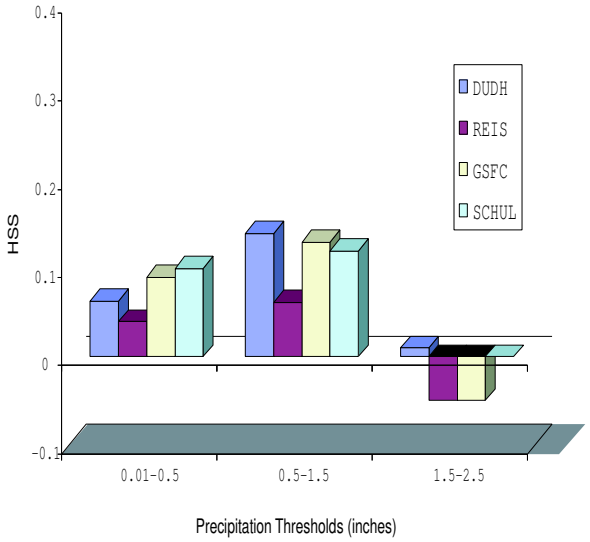

Figure 7: Heideke skill scores for the defined precipitation classes (in) for different microphysical schemes for the 4.5-km domain.

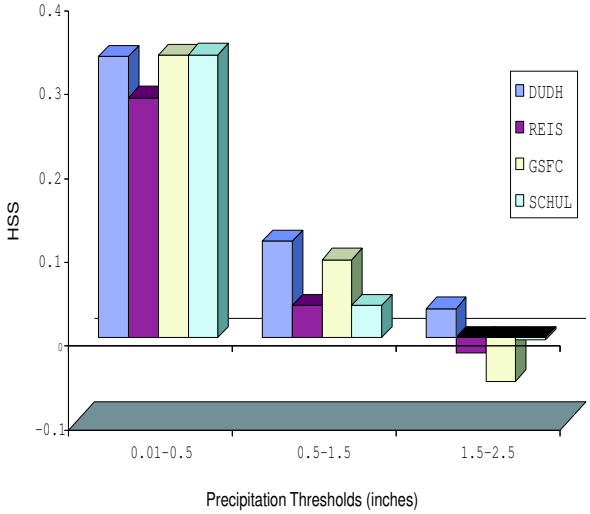

Figure 8: As in Fig. 7 but for the 1.5-km domain.

classes, whereas BIAS is larger than one (1.2–1.3) for the moderate class and much smaller than one (0.6–0.7) for the light precipitation class.

Among the four selected microphysical parameterizations, REIS has the best overall performance and the highest skill compared to the other schemes. Comparing the 24-h precipitation amounts obtained at 4.5-km resolution by REIS to that obtained by other schemes, we find that DUDH and GSFC schemes place significantly more precipitation on the lee slopes, which is reflected in their weak lee-side QPF skill scores. The likely source of these errors is in small fall speeds leading to the rapid advection of hydrometeors to the lee side. Additionally, DUDH produced more rain water than the other schemes on both the windward and lee slopes. Looking at the windward and lee slopes separately, we find that the DUDH performance is better on the windward than on the lee side. Conversely, SCHUL shows a worse performance on the windward compared to the lee side. Among the schemes that include graupel production, REIS and SCHUL showed increased production of cloud water content and graupel near the crestline, compared to GSFC which predicts more graupel production on the lee side.

At 1.5-km resolution, the difference in predicted 24-h precipitation amounts between any two microphysical schemes were larger compared to that obtained at the lower resolution. Particularly large differences were obtained with DUDH scheme compared to the other schemes.

5. SUMMARY

We have examined the skill of the MM5 model in predicting orographic precipitation for high-impact wintertime precipitation events in the Sierra Nevada, and the sensitivity of that skill to the choice of the microphysical parameterization and horizontal resolution. The performance of four existing microphysical schemes in MM5 (DUDH, REIS, GSFC, SCHUL) was examined in this study. The verification data set consists of ground precipitation measurements obtained at 15-min intervals during a selected number of wintertime storms documented during the SCPP experiment in the 1980's. For the verification purposes, the measured and predicted precipitation amounts within a given 24-h forecast period were divided into light (0.01–0.5 in), moderate (0.5–1.5 in), and heavy (1.5–2.5) precipitation classes.

Our results show the tendency of the existing microphysical schemes in MM5 to produce overprediction of precipitation on both the windward and lee slopes of the Sierra Nevada. Irrespective of the choice of the microphysical scheme, the highest QPF skill is displayed for the moderate precipitation amounts (0.5–1.5 in), especially on the windward Sierra Nevada slopes. In agreement with earlier studies, we find that the QPF skill is not simply improved by increasing the horizontal resolution as

this, for example, leads to under-prediction of light amounts of precipitation downwind of the barrier and over-prediction of heavy precipitation amounts on both the upwind and lee-side slopes.

Among the four microphysical parameterizations included in our study, we find that REIS overall performed better than the other schemes on both sides of the barrier. All microphysical schemes produced more of daily total precipitation than observed, with much larger amounts on the windward slopes. In spite of large differences in the degree of sophistication in the representation of microphysical processes, both DUDH and GSFC display weak QPF skill by placing more precipitation on the lee slopes than the other schemes, with hydrometeors being rapidly advected to the lee side. The production of graupel near the crestline was much higher in REIS and SCHUL compared to GSFC, in which all hydrometeors were too readily advected to lee side. The high-resolution simulations at 1.5-km resolution generally increased the noted differences between the 24-h forecasted precipitation amounts obtained by these four microphysical schemes.

Acknowledgments. This research has been supported by the National Science Foundation (NSF), Division of Atmospheric Sciences, Grant ATM–9908995.

6. REFERENCES

Bruintjes, R. T., T. L. Clark, and W. D. Hall, 1996: Interactions between topographic airflow and cloud/precipitation development during the passage of a winter storm in Arizona, *J. Atmos. Sci.*, **51**, 48–67.

Cayan, D. R. and L. Riddle, 1993: Atmospheric circulation and precipitation in the Sierra Nevada. Proceedings of the AWRA 28th Annual Conference and Symposium, Reno, Nevada, Nov 1-5, 1992, *Managing Water Resources During Global Change*, R. Herrmann, Ed, 711–720.

Colle, B. A., and C. F. Mass, 2000: The 5-9 February 1996 flooding event over the Pacific northwest: Sensitivity studies and evaluation of the MM5 precipitation forecasts. *Mon. Wea. Rev.*, **128**, 593–617.

Colle, B. A., and C. F. Mass, D. Ovens, M. Albright, and K. Westrick, 2002: Does Increasing Horizontal Resolution Produce Better Forecasts?: The Results of Two Years of Real-Time Numerical Weather Prediction in the Pacific Northwest. *Bull. Amer. Meteor. Soc.*, **83**, 407–430.

Cressman, G. P., 1957: An operational objective analysis system. *Mon. Wea. Rev.*, **87**, 367–374.

Dudhia, J., 1989: Numerical study of convection observed during the winter monsoon experiment using a mesoscale two-dimensional model. *J. Atmos. Sci.*, **46**, 3077–3107.

Fritsch, J. M., and Coauthors, 1998: Quantitative precipitation forecasting: Report of the eighth prospectus development team, U.S. Weather Research Program. *Bull. Amer. Meteor. Soc.,* **79**, 285–299.

Gaudet, B., and W. R. Cotton, 1998: Statistical characteristics of real-time precipitation forecasting model. *Wea. Forecasting*, **13**, 966–982.

Grell, G. A., J. Dudhia, and D. R. Stauffer, 1994: Description of the Fifth-generation Penn State/NCAR Mesoscale Model (MM5). NCAR Tech. Note TN-398. 128 pp.

Hemmer, G. L., and Coauthors, 1987: SCPP meteorological and statistical support. Interim Progress Rep. 1986-87.

Hsie, E.-Y., R. A. Anthes, and D. Keyser, 1984: Numerical simulation of frontogenesis in a moist atmosphere, *J. Atmos. Sci.*, **41**, 2581–2594.

Kessler, E., 1969: On the distribution and continuity of water substance in atmospheric circulations. Meteorol. Monogr. No. 10, American Meteorological Society, Boston, USA.

Lin, Y.-L., R. D. Farley, and H. D. Orville, 1983: Bulk parameterization of the snow field in a cloud model. *J. Clim. Appl. Meteorol.*, **22**, 1065–1092.

Marzban, C., 1998: Scalar measures of performance in rare-event situations. *Wea. Forecasting*, **13**, 753–763.

Montani, A., A. J. Thorpe, R. Buizza, and P. Unden, 1999: Forecast skill of the ECMWF model using targeted observations during FASTEX. *Quart. J. Roy. Meteor. Soc.*, **125**, 3219–3240.

Rauber, R. M., 1992: Microphysical structure and evolution of a Sierra Nevada shallow orographic cloud system. *J. Appl. Meteor.*, **31**, 3–24.

Reisner, J., R. M. Rasmussen, and R. T. Bruintjes, 1998: Explicit forecasting of supercooled liquid water in winter storms using MM5 mesoscale model. *Quart. J. Roy. Meteor. Soc.*, **124**, 1071–1107.

Reynolds, D. W., and A. S. Dennis, 1986: A review of the Sierra Cooperative Pilot Project. *Bull. Amer. Meteor. Soc.*, **67**, 513–523.

Schultz, P., 1995: An explicit cloud physics parametrization for operational numerical weather prediction. *Mon. Wea. Rev.*, **123**, 3331–3343.

Schultz, D. M., and Coauthors, 2002: Understanding Utah winter storms : The Intermountain Precipitation Experiment. *Bull. Amer. Met. Soc.*, **83**, 189–210.

Tao, W.-K., and J. Simpson, 1993: Goddard Cumulus Ensemble Model, Part I: Model Description. *Terrestrial, Atmospheric and Oceanic Sciences*, **4**, 35–72.

Wilks, D., 1995: *Statistical Methods in Atmospheric Sciences : An Introduction.* Academic Press, 467 pp.